

Article

Path Planning of Hydraulic Support Pushing Mechanism Based on Extreme Learning Machine and Descartes Path Planning

Suhua Li ¹, Jiacheng Xie ¹, Xuewen Wang ^{1,*}, Fang Ren ¹, Xin Zhang ¹ and Qingbao Bao ²

¹ Shanxi Key Laboratory of Fully Mechanized Coal Mining Equipment, College of Mechanical and Vehicle Engineering, Taiyuan University of Technology, Taiyuan 030024, China; lisuhua0063@link.tyut.edu.cn (S.L.); xiejiacheng@tyut.edu.cn (J.X.); renfang@tyut.edu.cn (F.R.); zhangxin0035@link.tyut.edu.cn (X.Z.)

² State Key Laboratory of Mining Equipment and Intelligent Manufacturing, Taiyuan 030024, China; tzmjbaoqingbao@163.com

* Correspondence: wangxuewen@tyut.edu.cn

Abstract: As a floating system connecting hydraulic support and scraper conveyor, the path planning of pushing mechanism is of great significance for their coordinated movement. In this paper, a method for path planning of hydraulic support pushing mechanism based on extreme learning machine (ELM) and Descartes path planning is proposed. According to the motion characteristics of moving mechanism, it is transformed into industrial robot model, based on the characteristics of the coordinates of the key points on the ear seat of the scraper conveyor when advancing, a prediction method of the key points coordinates based on ELM is proposed, so the target location of the end-effector is obtained. The path of the joint is determined by polynomial path partition and Descartes path planning method. The path is modified by Gaussian filtering method, and the peak value of path obtained by planning is filtered out, and the path correction is realized. Finally, the virtual simulation test is carried out in Unity3D. The planned coordinate curve has Poisson-like distribution and approximately around the target coordinate curve, and local error and correction error are within 2 cm and 0.1 cm, respectively. The coordinate curve obtained by combining planning and correction has a better effect.

Keywords: virtual reality; Unity3D; scraper conveyor; hydraulic support; pushing mechanism; path planning



Citation: Li, S.; Xie, J.; Wang, X.; Ren, F.; Zhang, X.; Bao, Q. Path Planning of Hydraulic Support Pushing Mechanism Based on Extreme Learning Machine and Descartes Path Planning. *Symmetry* **2021**, *13*, 97. <https://doi.org/10.3390/sym13010097>

Received: 19 December 2020

Accepted: 4 January 2021

Published: 8 January 2021

Publisher's Note: MDPI stays neutral with regard to jurisdictional claims in published maps and institutional affiliations.



Copyright: © 2021 by the authors. Licensee MDPI, Basel, Switzerland. This article is an open access article distributed under the terms and conditions of the Creative Commons Attribution (CC BY) license (<https://creativecommons.org/licenses/by/4.0/>).

1. Introduction

With the advancement of intelligent mining [1,2] and the application of Digital Twin technology [3] in the coal mine field, virtual reality (VR) technology [4,5] is used to preview and explore problems in the mining process, which provides ideas for solving related problems. The collaboration between hydraulic support and scraper conveyor is one of the key technologies in the “three machines” collaboration of fully mechanized coal-mining face in virtual environment [6–8], and implementing collaborative promotion of hydraulic support and scraper conveyor in a virtual environment is one of the key technologies to realize digital twin fully mechanized coal-mining face.

Cooperative promotion of hydraulic support and the scraper conveyor is mainly reflected in the shearer cutting triangular coal, hydraulic support needs to push scraper conveyor into S type [9–12], straightness of the scraper conveyor [13–18], reasons for and control problems of creeping of fully mechanized coal-mining face [19–21], and propelling problems of hydraulic support and scraper conveyor in pitching [22]. It can be seen that the collaboration between hydraulic support and scraper conveyor runs through the whole process of coal mining in the fully mechanized coal-mining face, so it is urgent to realize collaborative movement between the hydraulic support and scraper conveyor in a virtual environment, laying a foundation for the collaboration of three machines in a fully-mechanized coal mining face under a VR environment.

As a floating connecting mechanism connecting the hydraulic support and scraper conveyor, the movement of the pushing mechanism is the hub to realize the cooperation between the hydraulic support and scraper conveyor (in this paper, the floating connection mechanism connecting the hydraulic support and scraper conveyor is called the ‘floating connection mechanism’). The floating connection mechanism is transformed into an industrial robot model, and its motion planning can realize the accurate capture of the key points of the translation ear base of the scraper conveyor in the virtual environment when its specific motion is unknown, so as to realize the hydraulic support to push the scraper conveyor more accurately, which provides a new way for the virtual collaboration between the hydraulic support and the scraper conveyor. Unity3D is a multi-dimensional virtual simulation engine [23], it can not only realize dynamic visualization of various complex working conditions, and it can also be applied as a solver to solve complex problems and output data in real time. At present, relevant scholars [24–27] have carried out simulation research on related work in coal mining by using Unity3D, and obtained real and reliable simulation research results, so Unity3D can be used for related research.

In this paper, aiming at the collaborative problem of hydraulic support and scraper conveyors, this paper focuses on the path planning of the pushing mechanism, and proposes a path planning method of the hydraulic support pushing mechanism based on the extreme learning machines (ELM) algorithm [28,29] and Cartesian path planning [30]. According to the motion characteristics of the pushing mechanism, it is transformed into an industrial robot model. Based on the time sequence characteristics of the coordinates of the key points on the translation ear base in the middle trough, a prediction method of the key point coordinates based on ELM is proposed, and the target point position of the end-effector of the equivalent manipulator model is obtained. Based on the predicted position of the target point, the path of the joint of the floating connection mechanism is determined by the polynomial path segmentation technology and the Cartesian path planning method; Gaussian filtering method is used to filter out the peak value in the path obtained by planning, and the path of floating connection mechanism is modified to obtain the final planning path.

2. Overall Framework

Because of the similarity between the motion characteristics of the floating connection mechanism and industrial robot, the viewpoint of the industrial robot is introduced to solve the motion analysis of the floating connection mechanism.

The motion of the floating connection mechanism is closely related to the position and posture of the connected equipment, so it is necessary to integrate the position relationship of scraper conveyor and hydraulic support when planning its path. The overall framework of the paper is shown in Figure 1.

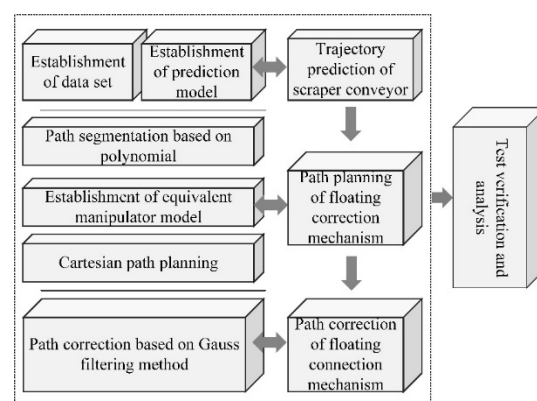


Figure 1. Overall framework.

3. Trajectory Prediction of End-Effector in Equivalent Manipulator Model of Floating Connection Mechanism

Because the movement of the floating connection mechanism is affected by the cutting information of the shearer, the fluctuation of the coal seam floor and the position and posture of the scraper conveyor, the movement of the end-effector of the equivalent manipulator model of the floating connection mechanism is unknown. In the process of coal mining, when the hydraulic support pushes the scraper conveyor on the coal seam floor, the translation ear base of the middle trough of the scraper conveyor is the action position of the pushing mechanism, and the key point on the push ear socket is the capture position of the end-effector of the equivalent manipulator model of floating connection mechanism, so it is necessary to predict its trajectory based on the existing data of the scraper conveyor.

3.1. Establishment of the Dataset

The dataset is derived from the virtual environment created in Unity3D, which represents the position coordinates of the pushing point on the translation ear base. The number of hydraulic support in virtual scene is $yyzz_Num$ ($Num \in (1,11)$), the number of the middle trough of scraper conveyor is ZBC_Num ($Num \in (1,13)$), through the following program, the position coordinates of each middle trough are output in the format of XML in Unity3D, and the detection results of the sensor for the position detection of the middle trough are simulated by the following functions.

```
gameobject_Position_x = this.transform.position.x;
gameobject_Position_y = this.transform.position.y;
gameobject_Position_z = this.transform.position.z;
```

3.2. Extreme Learning Machines Model

ELM is a kind of feedforward neural network, which has good generalization performance and extremely fast learning ability [31]. ELM does not need to adjust the weight based on gradient back propagation, but sets the weight through Moore Penrose generalized inverse. Its internal structure is shown in Figure 2.

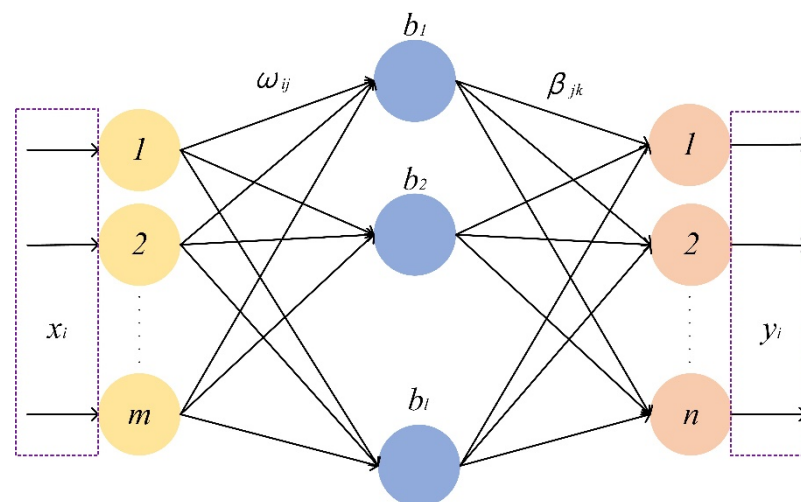


Figure 2. Internal structure of ELM.

ELM has three main structures: input layer, hidden layer, and output layer. It has the advantages of strong generalization ability and avoiding over fitting [24]. Assuming that there are n arbitrary samples, its neural network model is

$$f_L(x) = \sum_{i=1}^L \beta_i g(x) = \sum_{i=1}^L \beta_i g(W_i x_j + b_i), j = 1, \dots, N \quad (1)$$

where $\beta_i = [\beta_{i1}, \beta_{i2}, \beta_{i3}, \dots, \beta_{in}]$, $W_i = [w_{i1}, w_{i2}, w_{i3}, \dots, w_{in}]$, L is the number of hidden units, N is the number of training samples, β is the weight vector between the hidden layer and output layer, W is the weight vector between the input layer and hidden layer, $g(x)$ is the activation function, and b is the offset vector.

The objective of single hidden layer neural network learning is to minimize the output error, which can be expressed as Equation (2).

$$\sum_{i=1}^L \beta_i g(X_j + b_i) = t_j, j = 1, \dots, N \quad (2)$$

The above equation can also be expressed as a matrix $H\beta = T$, where H is the output of hidden layer nodes, β is the output weight, and T is the expected output. In order to train the single hidden layer neural network, we hope to get W_i^{-1} , b_i^{-1} and β_i^{-1} to make the Equation (3) hold.

$$\|H(W_i^-, b_i^-)\beta_i^- - T\| = \min_{W, b, \beta} \|H(W_i^-, b_i^-)\beta_i^- - T\|, i = 1, 2, \dots, L \quad (3)$$

This is equivalent to the minimization loss function as Equation (4).

$$E = \sum_{j=1}^N \left[\sum_{i=1}^L \beta_i g(W_i X_j + b_i) - t_j \right]^2 \quad (4)$$

In ELM, once the input weight and the offset of hidden layer are determined randomly, the output matrix of hidden layer is uniquely determined. The trained single hidden layer neural network can be transformed into solving a linear system. The output weight can be determined as the Equation (5).

$$\beta^- = H^* T \quad (5)$$

where H^* is the generalized inverse matrix.

3.3. Model Evaluation Index

Mean square error (MSE) and coefficient of determination (R^2) are used as evaluation indexes of simulation deviation, which are used to reflect the difference between measured and simulated values and the fitting effect of the model.

$$MSE = \frac{1}{N} \sum_{i=1}^N (y_i - \hat{y}_i)^2 \quad (6)$$

$$R^2 = 1 - \frac{\sum_{i=1}^N (\hat{y}_i - y_i)^2}{\sum_{i=1}^N (\bar{y} - \bar{y}_i)^2} \quad (7)$$

Among them, N are the sample capacity, y_i and \hat{y}_i are the measured and predicted values of the track coordinates of the scraper conveyor, respectively.

3.4. Comparison of Prediction Model Algorithms

In order to select the prediction algorithm with high prediction performance, back propagation neural network (BP neural network), support vector machine (SVM), ELM are selected, RMSE, and R^2 are used as evaluation indexes. The data set of this section adopts the actual drum cutting height obtained from a coal mine in Shanxi, China, with a total of 17×39 sequences. This section uses the cutting height of the first 16 knives to predict the cutting height of the 17th knife.

It can be seen from Figure 3 that the prediction results based on ELM have high precision; as can be seen from Table 1, the MSE value and R^2 value of the prediction results based on ELM prediction algorithm are the smallest and the largest respectively, which

means that the error between the predicted value and the actual value is the smallest. Consequently, the ELM algorithm selected in this paper has a better prediction effect.

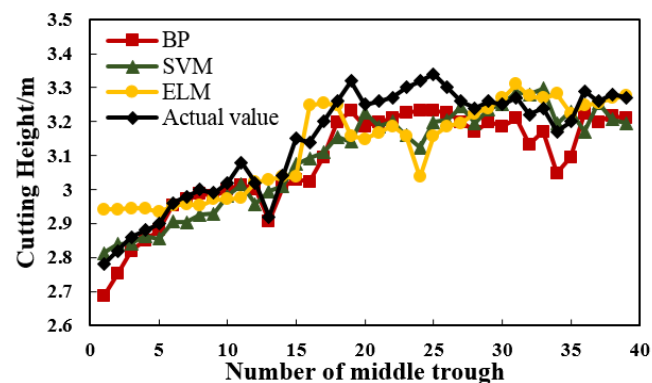


Figure 3. Comparison of prediction results.

Table 1. Prediction model evaluation results.

Algorithm Name	MSE	R^2
BP neural network	0.005873	0.83075
SVM	0.005966	0.783805
ELM	0.0054874	0.97151

4. Path Planning of the End-Effector of The Equivalent Manipulator Model of Floating Connection Mechanism

The floating connection mechanism can change the motion behaviour of each degree of freedom according to the position of the scraper conveyor, which has the general characteristics of industrial robots. Therefore, the floating connection mechanism can be transformed into an industrial robot model for research. Due to the uncertainty of the motion of industrial robot, it is necessary to plan the path based on the space dimension and time dimension. Figure 4 shows the path planning diagram of the converted manipulator and the key point location map that the end-effector needs to capture.

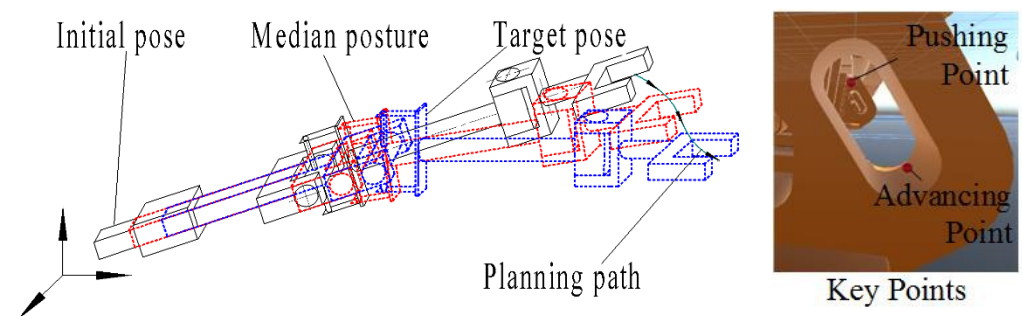


Figure 4. Schematic diagram of robot path planning.

4.1. Establishment of Equivalent Manipulator Model of Floating Connection Mechanism

The motion of floating connecting mechanism is spatial motion, including the extension of piston rod, pitching and yawing of relay bar, and yaw motion of joint, and the joint motion of industrial robot [30] includes linear motion, pitch motion, yaw motion, and roll motion. It can be seen that the motion of floating connection mechanism is consistent with the motion characteristics of industrial robot. Therefore, the floating connection mechanism can be transformed into an industrial robot manipulator model to study its motion law. The transformation model and D–H coordinate system are shown in Figure 5, and the meanings of parameters in the coordinate system are shown in Table 2.

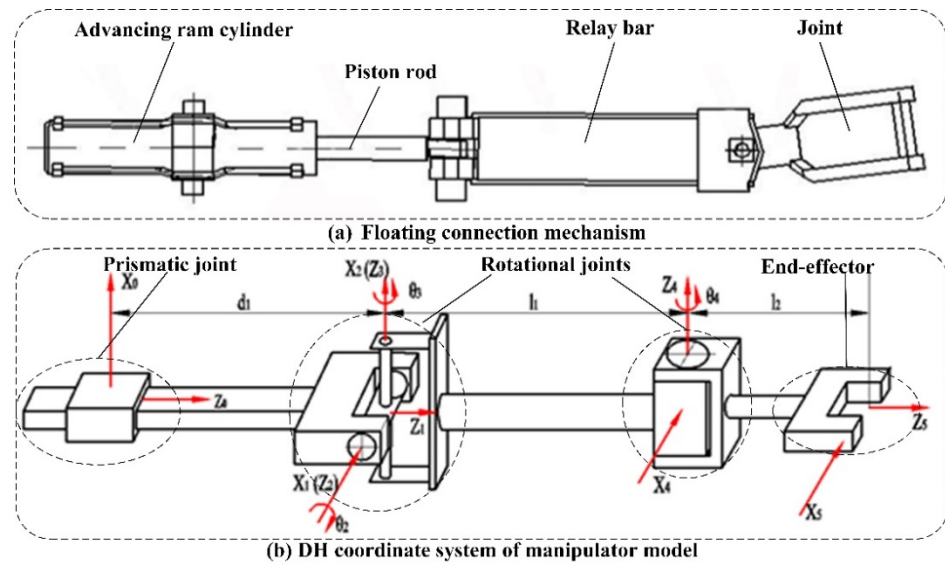


Figure 5. Transformation model and D–H coordinate system.

Table 2. Motion parameters.

Symbol	Name	Meaning
$x_i - z_i$	Reference system	Local reference system assigned to each joint
θ_i	Articular angle	Angle of rotation of the x_{i-1} axis around the x_i axis
d_i	Articular distance	Distance between x_{i-1} axis and x_i axis along z_{i-1} axis
a_i	Length of linkage	Distance between z_{i-1} axis and z_i axis along x_i axis
α_i	Torsion angle of linkage	Rotation angle of z_{i-1} axis around x_i axis
l_1	Length of the relay bar	
l_2	Length of the joint	

4.2. Path Segmentation Technology

When the initial position and final position of the end-effector are known, the whole path of the end-effector of the equivalent manipulator model can be divided into some segments [30], and the whole trajectory formula can be obtained by splicing a series of low-order polynomials.

In general, the path of a polynomial of degree n is shown in Equation (8).

$$q(t) = a_0 + a_1t + a_2t^2 + \dots + a_nt^n \tag{8}$$

A total of $n + 1$ conditions are required to solve the equation. The Equation (8) is solved and smoothed by finite derivation of known points, locations, velocities, accelerations, and other equations.

The following boundary conditions should be considered in the whole trajectory: $q(t_0) = q_0, \dot{q}(t_0) = 0, \ddot{q}(t_0) = 0, q(t_1) = q_1, q(t_2) = q_2, q(t_3) = q_3, q(t_4) = q_4, \dot{q}(t_4) = 0, \ddot{q}(t_4) = 0$. Divide the path into the following four segments: $q_1(t), q_2(t), q_3(t)$ and $q_4(t)$, and the details are shown in Table 3.

$$\begin{cases} q(t_0) < q_1(t) < q(t_1), t_0 < t < t_1 \\ q(t_1) < q_2(t) < q(t_2), t_1 < t < t_2 \\ q(t_2) < q_3(t) < q(t_3), t_2 < t < t_3 \\ q(t_3) < q_4(t) < q(t_4), t_3 < t < t_4 \end{cases} \tag{9}$$

Table 3. Path fragment.

Path Fragment	Polynomial	Range	Independent Variable	Boundary Conditions
$q_1(t)$	$q_1(t) = a_0 + a_1(t - t_0) + a_2(t - t_0)^2 + a_3(t - t_0)^3$	$q(t_0) < q(t) < q(t_1)$	$t_0 < t < t_1$	$q_1(t_0) = q_0$ $\dot{q}_1(t_0) = 0$ $\ddot{q}_1(t_0) = 0$ $q_1(t_1) = q_1$
$q_2(t)$	$q_2(t) = b_0 + b_1t + b_2t^2$	$q(t_1) < q_2(t) < q(t_2)$	$t_1 < t < t_2$	$q_2(t_1) = q_1$ $\dot{q}_2(t_1) = \dot{q}_1(t_1)$ $q_2(t_2) = q_2$
$q_3(t)$	$q_3(t) = c_0 + c_1t + c_2t^2$	$q(t_2) < q_3(t) < q(t_3)$	$t_2 < t < t_3$	$q_3(t_2) = q_2$ $\dot{q}_3(t_2) = \dot{q}_2(t_2)$ $q_3(t_3) = q_3$
$q_4(t)$	$q_4(t) = d_0 + d_1t + d_2t^2 + d_3t^3 + d_4t^4$	$q(t_3) < q_4(t) < q(t_4)$	$t_3 < t < t_4$	$q_4(t_3) = q_3$ $\dot{q}_4(t_3) = \dot{q}_3(t_3)$ $q_4(t_4) = q_4$ $\dot{q}_4(t_4) = 0$ $\ddot{q}_4(t_4) = 0$

According to the analysis of the above boundary conditions, the path planning of the end-effector of the equivalent manipulator model of floating connection mechanism can be studied in a certain direction.

4.3. Cartesian Path Planning

If the manipulator moves from point $P_1(x_{p1}, y_{p1}, z_{p1})$ to point $P_2(x_{p2}, y_{p2}, z_{p2})$ in a certain period of time, the linear relationship between point P_1 and point P_2 is established according to the function expression of x coordinate related to time change, and the function expression of y and z coordinate with respect to time variable is obtained.

$$y = y_{p1} + \frac{y_{p2} - y_{p1}}{x_{p2} - x_{p1}}(x - x_{p1}) \quad (10)$$

$$z = z_{p1} + \frac{z_{p2} - z_{p1}}{x_{p2} - x_{p1}}(x - x_{p1}) \quad (11)$$

The position coordinates of the end-effector of the manipulator are obtained, and the function expression of the joint variables with respect to the time variables can be obtained by using the motion law of the joint variables obtained by inverse kinematics.

5. Motion Path Optimization Based on Gaussian Filter Correction

Due to the uncertainty of the motion of floating connection mechanism and the limitation of the position between the hydraulic support and scraper conveyor, most of the trajectories fluctuate in a reasonable range, but there are some errors between the planned trajectory and actual trajectory. Gaussian filtering is a kind of linear filtering, which can filter the data of high probability occurrence area for weighted average, and take its arithmetic mean value as filtering output, which can effectively suppress the noise obeying normal distribution [32].

$$f(t) = \frac{1}{\sqrt{2\pi}\sigma} e^{-\frac{(t-\mu)^2}{2\sigma^2}} \quad (12)$$

$$\mu = \sum_{i=1}^n \frac{t}{n} \quad (13)$$

$$\sigma = \sqrt{\frac{\sum_{i=1}^n (t - \mu)}{n - 1}} \quad (14)$$

The whole planning trajectory can be regarded as the splicing of multiple Gaussian functions, so it is necessary to modify each path segment, i.e., Gaussian correction should be applied to the places where the planning trajectory fluctuates greatly. The correction function $R(x)$ is shown in Equation (15).

$$R(x) = q(t) - (1 - \frac{1}{k}f(t)) \quad (15)$$

where k is the number of path fragments.

6. Establishment of Virtual Planning Space Based on Unity3D

In the trajectory planning of the equivalent robot model of floating connection mechanism, it is necessary to establish the high-fidelity motion space of floating connection mechanism—i.e., to visualize the environment of the connected equipment—and to carry out path planning according to the relative position and posture changes of the hydraulic support and the corresponding middle trough.

6.1. Construction of Virtual Coal Seam Floor Based on Reverse Reconstruction Technology

Due to the influence of uneven basement in the process of coal seam deposition and the later geological structure movement, the situation of large fluctuation of coal seam floor appears [33,34]. In this paper, the coal seam floor with dip angle of 10° and undulation along the longitudinal advancing direction is selected for research.

Establish the 3D model of the target in UG, import it into 3DMAX in STL format, convert it into FBX format and import it into Unity3D, and get the coal seam floor under virtual environment [34], as shown in Figure 6.

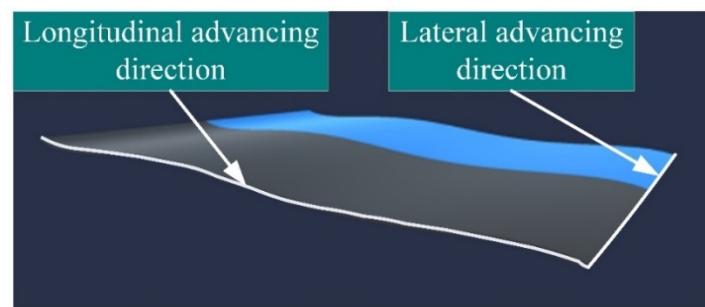


Figure 6. Virtual coal seam floor.

6.2. Parameter Setting of Coal Mining Equipment

In order to establish the mapping relationship between virtual environment and physical environment, it is necessary to parameterize configuration of coal mining equipment in virtual environment. The conversion ratio between Unity3D and actual space is 100:1. The specific parameter configuration results are shown in Table 4.

Table 4. Parametric setting table.

Name	Model	Research Object	Theoretical Value	Actual Value (In Unity3D)
Hydraulic support	ZY11000/18/38D	Base	About 7700 Kg	About 77 Kg
Scraper conveyor	MG400/920-WD	Middle trough	153 Kg	1.53 Kg
Middle trough spacing	—	Adjacent middle trough	$l = \frac{\pi r}{360}$	0.216 cm

6.3. Establishment of Virtual Contact Model

The Physical Engine in Unity3D can realize the establishment of physical relationship constraints of virtual model, and the role of the relevant physical engine is shown in Table 5. As shown in Figure 7, on the basis of completing the parameter configuration, a series of physical engines [35] are installed on the virtual model to realize the establishment of physical relations such as the gravity of coal mining equipment, the friction between coal mining equipment and coal seam, the force between coal mining equipment and air, and the force between coal mining equipment; the joint components in Unity3D are used to simulate the effect of each middle trough of virtual scraper conveyor. The maximum bending angle of joint components is set, and the limit value of bending angle of adjacent middle troughs of scraper conveyor is set to realize real virtual conversion. When the coal mining equipment is advancing on the virtual coal seam, the physical engine has relative movement on different objects, and the physical engine on the equipment and the physical engine on the coal seam will have pressure changes.

Table 5. Role of relevant physical engines.

Name		Function
Rigidbody		Make the virtual object move under the control of physical system, and make the virtual object accept external force and torque to ensure that the motion of the object is the same as that of the real world.
Colliders	Box Collider Mesh Collider Capsule Collider	Use with Rigidbody components to trigger a collision that causes virtual objects to collide with each other, and in physical simulation rigid bodies that do not have collisions pass through each other.
Character Joint	Low Twist Limit	It is used to restrict the rotation angle of joints under different rotation axes. The values of Low Twist Limit and High Twist Limit are set to -4 and 4 respectively.
	High Twist Limit	

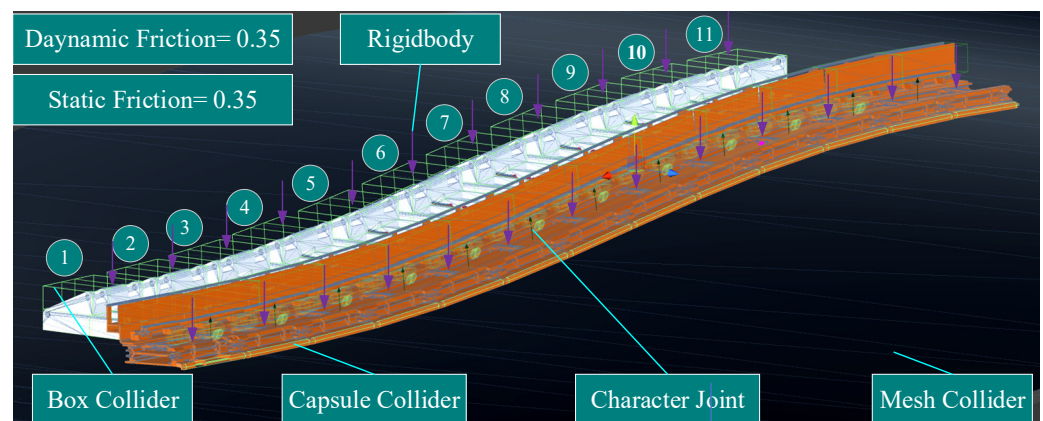


Figure 7. Coal mining equipment adaptive laying and related physical engine.

6.4. Establishment of Virtual Control Model

The `yyzzControl.cs` control script is installed on each hydraulic support, and the pushing and advancing support processes of hydraulic support is controlled by `PushingFunction` and `AdvancingFunction` respectively. The bending angle and propulsion process of the middle trough of each section is determined and represented by the script form of `GBJControl.cs`, which is installed on the parent object `GBJ` of the middle trough of the scraper conveyor. In the `yyzzControl.cs` script, `"GameObject.Find ("GBJ"). GetComponent<GBJControl>().gameObject1"` is used to realize the information sharing of the key points between the hydraulic support and scraper conveyor. The movement of the scraper conveyor is used as the trigger condition to trigger the movement of the pushing mechanism.

7. Research on Virtual Simulation and Analysis

In the virtual environment, the attitude of the scraper conveyor when the shearer is cutting forward is shifted to a given attitude. Based on the predicted position of the advancing point of the translation ear base as shown in Figure 4, the movement time of the scraper conveyor is recorded and displayed in real time by using the timing function of Unity3D, and the planned trajectory curve is obtained based on the contents of Sections 3.2 and 3.3. Because there is a certain error between the trajectory curve and the actual curve, it is necessary to modify the planned trajectory curve. When there is still a certain error between the modified trajectory and the actual trajectory curve, it can be corrected twice or more. Because the Cartesian path planning adopted in this paper expresses the other two coordinates according to the function expression of x-coordinate related to time change, the prediction algorithm in Section 2 is used to predict the position coordinates of the key points when the scraper conveyor moves the ear seat, i.e., to predict the x-coordinate of each key point.

7.1. Prediction and Application Results

The hydraulic support and scraper conveyor continuously advance 10 cycles. Ten cycles are predicted through the first nine cycles. The predicted results and the position curve of scraper conveyor are shown in Figure 8.

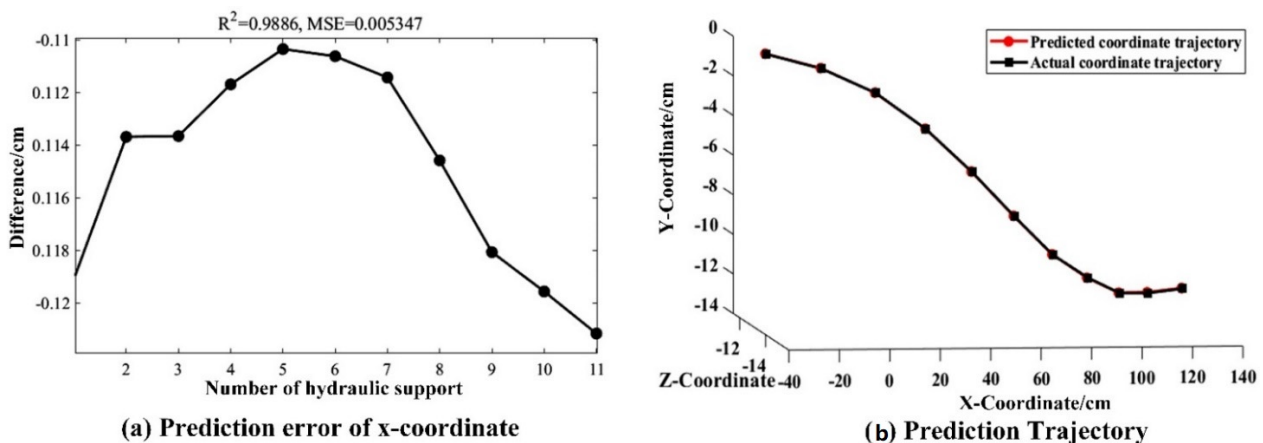


Figure 8. Prediction results.

From Figure 8, it can be seen that the R^2 value is between 0.98 and 0.99 and the MSE value is less than 0.01 respectively, which indicates that the trajectory predicted by ELM algorithm can be used as the basis of path planning.

7.2. Experimental Results Based on Joint Action of Trajectory Planning and Correction

Planning is based on the predicted data for the tenth cycle. No. 1 hydraulic support and corresponding middle trough are selected as the research objects. The lapse time is 0.33s and is divided into four periods: 0–0.06 s, 0.06–0.15 s, 0.15–0.24 s, and 0.24–0.33 s. The function relationship between the x value of the middle trough and time is calculated in the limited time period, and then the track curve of key point of the no. 1 hydraulic support connection can be obtained. According to the path planning method in Section 3, the coordinate planning trajectory of the equivalent end-effector of the floating connection mechanism is obtained as shown in Figure 9.

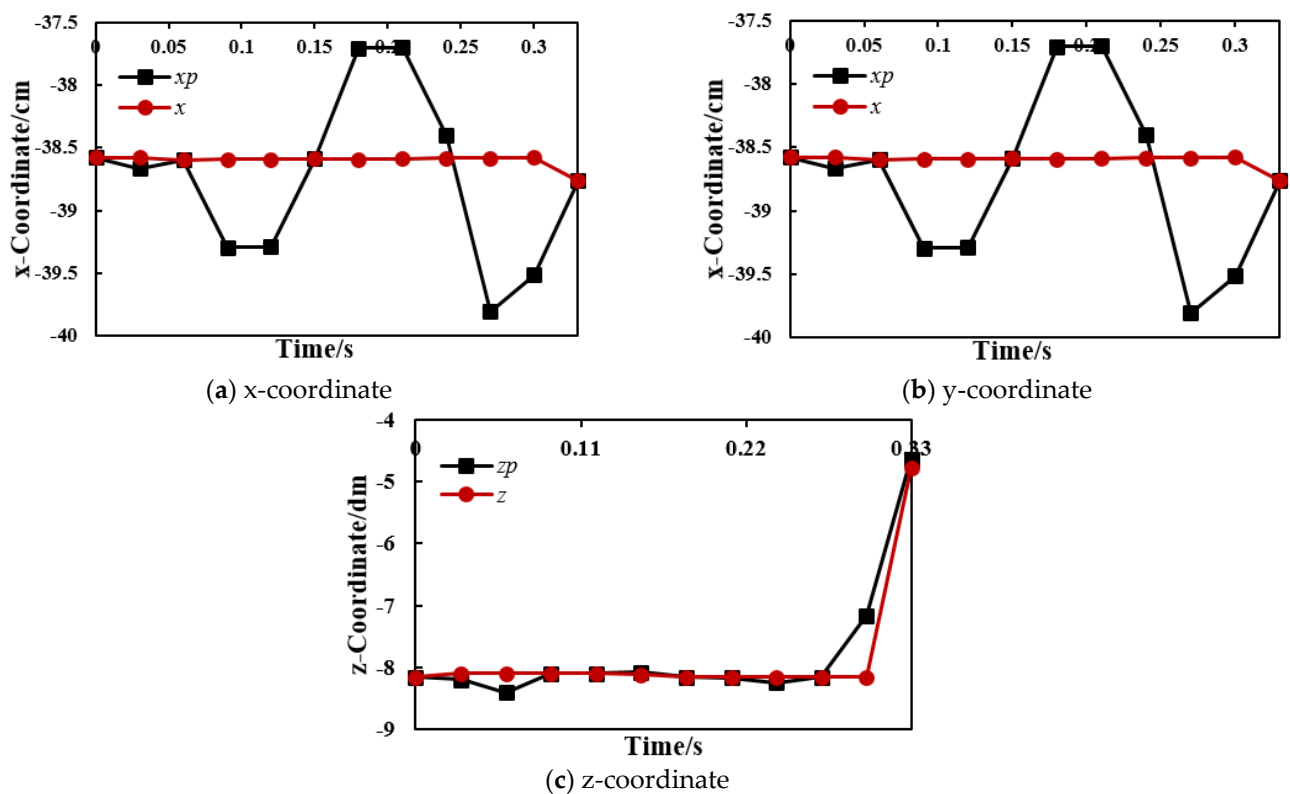


Figure 9. Coordinate planning trajectories of equivalent end-effector.

In Figure 9, x_p refers to the planned x value, x refers to the predicted value, and so does y and z . As can be seen from Figure 9, the coordinate curve of the planned equivalent end-effector of floating connection mechanism fluctuates around the actual x -coordinate curve. The error between the planned x -coordinate and actual trajectory fluctuates greatly, the maximum error is within 1.3 cm, and the planning trajectory has a phenomenon of Poisson distribution, which leads to the peak value of the planning curve of the x -coordinate; The planned y -coordinate value and z -coordinate values have the same change trend as the actual value, and the maximum local error is 2 cm and 1 cm, respectively. Therefore, it is necessary to correct the local error.

From Figure 10, it can be seen that the theoretical values of planned x -coordinates have peaks between 0.06–0.15 s, 0.15–0.24 s, and 0.24–0.3 s. Therefore, filtering is required to reach the maximum difference between the planned and actual values within 0.1 cm. After the first correction, the maximum difference of the trajectory is 0.26 cm. According to the correction results, the second correction should be carried out within 0.06–0.12 s, 0.15–0.24 s, and 0.24–0.27 s, the maximum difference between the correction results and the actual values is 0.08 cm, which meets the requirements of the correction results. Taking x -value as variable, the Cartesian path planning and Gaussian filtering correction method are used to jointly modify the y -coordinate and z -coordinate, and the correction result is shown in Figure 11.

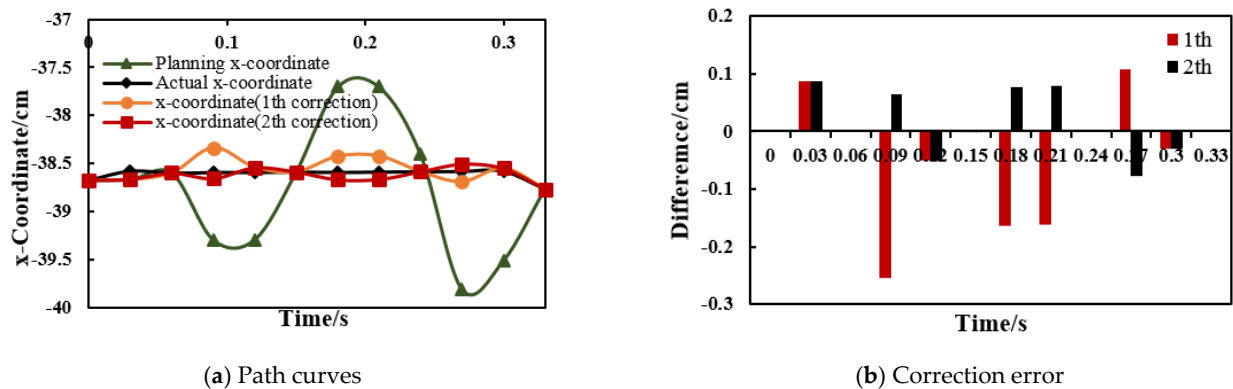


Figure 10. Corrected results and differences.

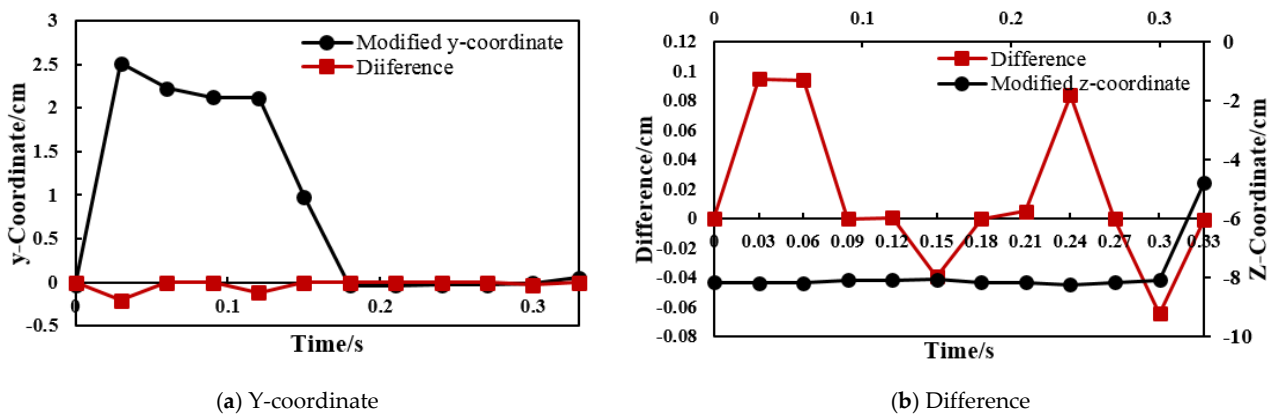


Figure 11. Corrected results and differences.

It can be seen from Figure 11 that the difference between the y -coordinate value and the z -coordinate value after the joint correction and the actual coordinate value is within 0.1 cm, and the difference is small, so the effect of joint correction is better. Therefore, the three-dimensional path curve of the end-effector can be determined by synthesizing the modified planning curve.

Applying the planned path to Unity3D, the path change of no. 1 hydraulic support corresponding to the middle trough is obtained; using the method proposed in this paper to plan the paths of all floating connecting mechanisms, the overall path changes of scraper conveyor can be obtained, as shown in Figure 12. By comparing the actual path curves with the predicted ones, the comparison results are shown in Figure 13.

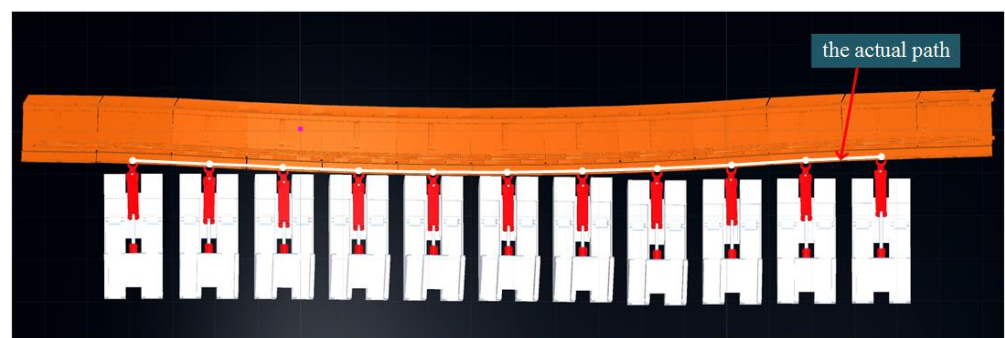


Figure 12. Attitude diagram of scraper conveyor.

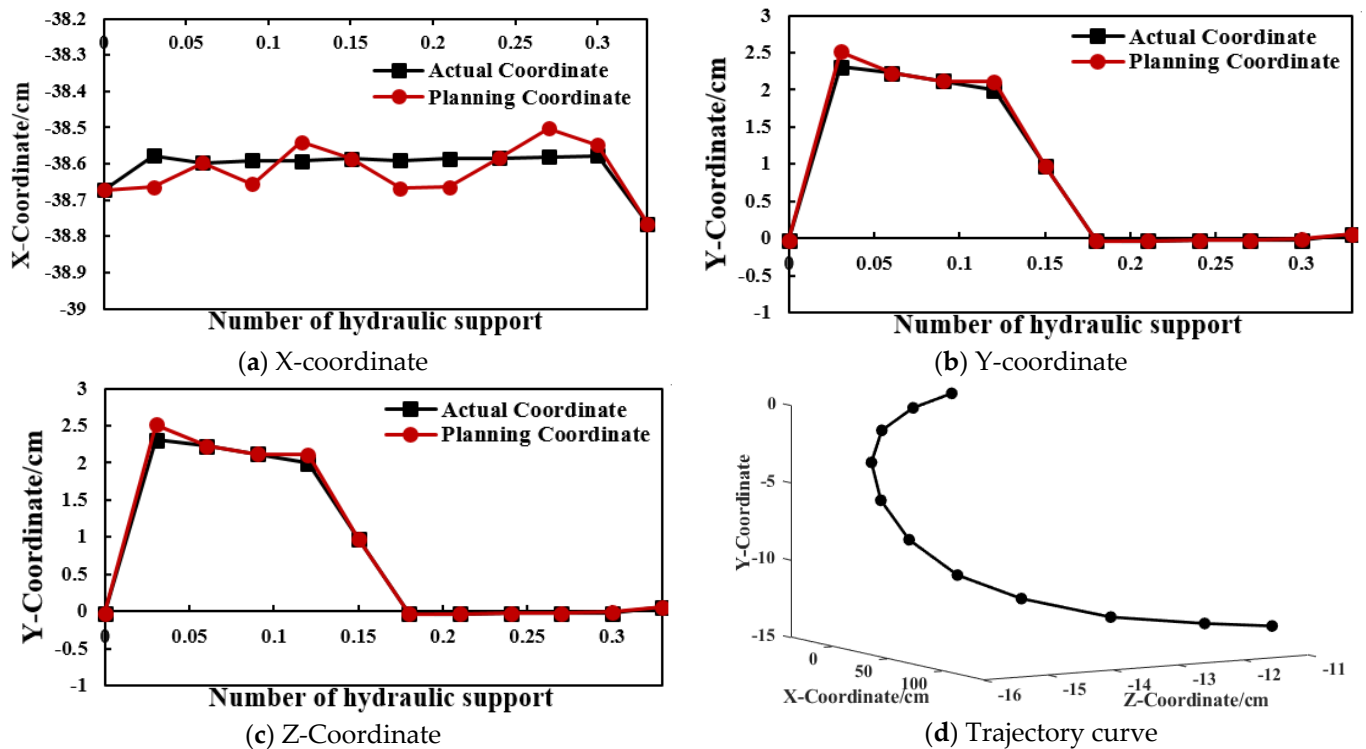


Figure 13. Single path planning and track diagram of scraper conveyor.

After applying the planned path to Unity3D, the error between the actual coordinate value and the planned coordinate value is within 0.01 cm, which is caused by the interaction between the physical engine of the equipment and coal seam floor when the scraper conveyor is laid on the virtual coal seam floor.

8. Conclusions and Prospect

In this paper, a method for path planning of hydraulic support pushing mechanisms based on ELM algorithm and Descartes path planning is proposed. The key points of scraper conveyor pushing ear are predicted, and the planning path of floating connection mechanism is finally obtained after joint planning and revision by Descartes path planning and Gauss filter correction method. This method is of great significance for realizing the cooperation between hydraulic support and scraper conveyor. This paper draws the following conclusions:

- (1) A virtual simulation space equivalent to path planning of pushing mechanism is established. Based on actual geological conditions, the virtual coal seam is established, and virtual coal machine equipment is parameterized according to production requirements. After installing a physical engine for virtual equipment and coal seam, a visual and highly reliable virtual simulation space is established.
- (2) The proposed path planning model has a good planning effect. On the premise of obtaining the predicted trajectory, when Cartesian path planning method is used for planning, the coordinate curve of the planned equivalent end actuator fluctuates roughly around the true curve, and the planned trajectory is similar to Poisson distribution, with the maximum local error within 2 cm, the overall planning effect is better.
- (3) The modified model proposed in this paper has a better effect. The peak value of the planned curve is filtered to achieve local correction. The simulation test proves that the corrected curve error is within 0.1 cm, and the modified model proposed in this paper has a good correction effect.

- (4) After the path planning is applied to the virtual environment, the error between the actual path and the planned path is small, and the error is within 0.01 cm. Consequently, the path planning method proposed in this paper can be used to preliminarily realize the cooperation between hydraulic support and scraper conveyor.

In the following research, it is necessary to plan the path of floating connection mechanism under more complex floor conditions, study the path characteristics of floating connection mechanism under different floor conditions, and finally establish the position relationship between hydraulic support and scraper conveyor according to the relevant depth prediction model.

Author Contributions: Conceptualization, S.L. and J.X.; Formal analysis, S.L.; Funding acquisition, X.W. and F.R.; Investigation, J.X.; Methodology, S.L.; Project administration, X.W.; Resources, X.W.; Software, J.X.; Supervision, X.W., F.R., X.Z., and Q.B.; Validation, X.W. and F.R.; Visualization, J.X.; Writing—original draft, S.L. All authors have read and agreed to the published version of the manuscript.

Funding: This research was supported by the National Natural Science Foundation of China (grant no. 52004174), Project funded by China Postdoctoral Science Foundation (no. 2019M651081), the Key Research and Development Program of Shanxi (201903D121141), the Natural Science Foundation of Shanxi Province (201901D211022), the Scientific and Technological Innovation Programs of Higher Education Institutions in Shanxi (no. 2019L0305), and Shanxi Postgraduate Innovation Project (2020SY552).

Institutional Review Board Statement: Not applicable.

Informed Consent Statement: Not applicable.

Data Availability Statement: Data available on request due to restrictions privacy. The data presented in this study are available on request from the corresponding author. The data are not publicly available due to laboratory regulations.

Acknowledgments: This research was supported by Shanxi Key Laboratory of Fully Mechanized Coal Mining Equipment and Virtual Reality Team of Fully Mechanized Mining.

Conflicts of Interest: The authors declare no conflict of interest. The funders had no role in the design of the study; in the collection, analyses, or interpretation of data; in the writing of the manuscript, or in the decision to publish the results.

References

1. Ralston, J.C.; Hargrave, C.O.; Dunn, M.T. Longwall automation: Trends, challenges and opportunities. *Int. J. Min. Sci. Technol.* **2017**, *27*, 733–739. [\[CrossRef\]](#)
2. Wang, J.; Huang, Z. The Recent Technological Development of Intelligent Mining in China. *Engineering* **2017**, *3*, 439–444. [\[CrossRef\]](#)
3. Xie, J.C.; Wang, X.W.; Hao, S.Q.; Yang, Z.Y. Virtual monitoring method for hydraulic supports based on digital twin theory. *Min. Technol.* **2019**, *128*, 77–87. [\[CrossRef\]](#)
4. Phillip, S.; Andrew, S.; Robert, S.; Etienne, V.W. Towards sustainable mixed reality simulation for the mining industry. *Min. Technol. Trans. Inst. Min. Metall.* **2019**, *128*, 246–254. [\[CrossRef\]](#)
5. Reid, D.; Ralston, J.; Dunn, M. Longwall Shearer Automation: From Research to Reality. In *Machine Vision and Mechatronics in Practice*; Billingsley, J., Brett, P., Eds.; Springer: Berlin/Heidelberg, Germany, 2015; pp. 49–57. [\[CrossRef\]](#)
6. Xie, J.C.; Wang, X.W.; Li, X.; Yang, Z.J. Research status and prospect of virtual reality technology in field of coal mine. *Coal Sci. Technol.* **2019**, *47*, 53–59. [\[CrossRef\]](#)
7. Foster, P.; Burton, A. Virtual reality in improving mining ergonomics. *J. S. Afr. Inst. Min. Metall.* **2004**, *104*, 129–133. [\[CrossRef\]](#)
8. Wang, X.W.; Xie, J.C.; Hao, S.Q.; Li, J.L.; Yang, Z.J.; Ren, F.; Bao, Q.B. Key technologies of real-time virtual monitoring method for an intelligent fully mechanized coal-mining face. *J. China Coal Soc.* **2020**, *45*, 1984–1996. [\[CrossRef\]](#)
9. Wang, C.; Li, W.; Yang, H.; Si, Z.Y.; Zhang, J.Y. Scraper conveyor shape detection based on dead reckoning. *J. China Coal Soc.* **2017**, *42*, 2173–2180. [\[CrossRef\]](#)
10. Liu, T.; Tan, C.; Wang, Z.; Xu, J.; Man, Y.; Wang, T. Horizontal Bending Angle Optimization Method for Scraper Conveyor Based on Improved Bat Algorithm. *Algorithms* **2019**, *12*, 84. [\[CrossRef\]](#)
11. Li, H.; Zhang, X. Calculation method of mathematical model on transverse bending movement of scraper in working Face. *J. China Coal Soc.* **2019**, *44*, 313–319. [\[CrossRef\]](#)
12. Xie, J.C.; Yang, Z.J.; Wang, X.W.; Wang, S.P.; Zhang, Q. Cooperative Solving Method of Chute Postures in the Bending Section of a Scraper Conveyor. *Adv. Mech. Eng.* **2018**, *10*, 1–13. [\[CrossRef\]](#)

13. Ralston, J.C.; Reid, D.C.; Dunn, M.T.; Hainsworth, D.W. Longwall automation: Delivering enabling technology to achieve safer and more productive underground mining. *Int. J. Min. Sci. Technol.* **2015**, *25*, 865–876. [[CrossRef](#)]
14. Hao, S.; Wang, S.; Malekian, R.; Zhang, B.; Liu, W.; Li, Z. A geometry surveying model and instrument of a scraper conveyor in unmanned longwall mining faces. *IEEE Access* **2017**, *5*, 4095–4103. [[CrossRef](#)]
15. Niu, J.F. Research of straightness control system of fully-mechanized coal mining face. *Ind. Mine Autom.* **2015**, *41*, 5–8. [[CrossRef](#)]
16. Wang, S.B.; He, Y.; Wang, S.J.; Zhang, B.Y.; Ge, S.R. Study on the alignment method and experiment of scraper conveyor. *J. China Coal Soc.* **2017**, *42*, 3044–3050. [[CrossRef](#)]
17. Wang, S.B.; Zhang, B.Y.; Wang, S.J.; Ge, S.R. Dynamic Precise Positioning Method of Shearer Based on Closing Path Optimal Estimation Model. *IEEE Trans. Autom. Sci. Eng.* **2018**, *16*, 1–8. [[CrossRef](#)]
18. Fang, X.Q.; Ning, Y.S.; Li, S.; Liang, M.F.; Wu, G.; Gu, C. Research on key technique of straightness perception of scraper conveyor based on fiber grating. *Coal Sci. Technol.* **2019**, *47*, 152–158. [[CrossRef](#)]
19. Song, X.; Wang, L.M. Research on Mining Engineering with Dual Gradient High Inclination-Angle Fully Mechanized Mining Technology. *Adv. Mater. Res.* **2014**, *977*, 231–234. [[CrossRef](#)]
20. Zhang, K.X.; Li, S.B.; He, M.C.; Ning, Y.; Zhang, L.; Huang, Z.H. Study on key technologies of intelligent unmanned coal mining series 1: Study on diagonal adjustment control technology of intelligent fully-mechanized coal mining face. *Coal Sci. Technol.* **2018**, *46*, 139–149. [[CrossRef](#)]
21. CSIRO. Creep Control. Available online: <http://www.lascautomation.com/dev/index.php/newoptimise/newcontrol/newcreepcontrol> (accessed on 4 December 2020).
22. Zhou, K.P. Complete equipment and technology for intelligent unmanned working face in thin coal seam. *Coal Sci. Technol.* **2020**, *48*, 59–67. [[CrossRef](#)]
23. Xie, J. Reaearch on key technologies base Unity3D game engine. In Proceedings of the 7th International Conferenece on Computer Science & Education (ICCSE 2012), Melbourne, Australia, 14–17 July 2012; pp. 695–699.
24. Xie, J.C.; Yang, Z.J.; Wang, X.W.; Wang, S.P.; Zhang, Q.; Michael, D. A Joint Positioning and Attitude Solving Method for Shearer and Scraper Conveyor under Complex Conditions. *Math. Probl. Eng.* **2017**, *2017*, 1–14. [[CrossRef](#)]
25. Li, J.L.; Liu, Y.; Xie, J.C.; Wang, X.W.; Ge, X. Cutting Path Planning Technology of Shearer Based on Virtual Reality. *Appl. Sci.* **2020**, *10*, 771. [[CrossRef](#)]
26. Shi, H.B.; Xie, J.C.; Wang, X.W.; Li, J.L.; Ge, X. An operation optimization method of a fully mechanized coal mining face based on semi-physical virtual simulation. *Int. J. Coal Sci. Technol.* **2020**, *7*, 147–163. [[CrossRef](#)]
27. Xie, J.C.; Yang, Z.J.; Wang, X.W.; Wang, Y.L. A remote VR operation system for a fully mechanized coal-mining face using real-time data and collaborative network technology. *Min. Technol.* **2018**, *127*, 1–11. [[CrossRef](#)]
28. Choudhary, R.; Shukla, S. A clustering based ensemble of weighted kernelized extreme learning machine for class imbalance learning. *Expert Syst. Appl.* **2021**, *164*, 114041. [[CrossRef](#)]
29. Du, P.; Wang, J.; Yang, W.; Niu, T. Point and interval forecasting for metal prices based on variational mode decomposition and an optimized outlier-robust extreme learning machine. *Resour. Policy* **2020**, *69*, 1–11. [[CrossRef](#)]
30. Ibrahim, A.H.; Claus, G.S.; Dionysis, B.; Ole, G. Field Robotics in Sports: Automatic Generation of guidance Lines for Automatic Grass Cutting, Striping and Pitch Marking of Football Playing Fields. *Int. J. Adv. Robot Syst.* **2011**, *8*, 113–121. [[CrossRef](#)]
31. Huang, G.B.; Zhou, H.; Ding, X.; Rui, Z. Extreme Learning Machine for Regression and Multiclass Classification. *IEEE Trans. Syst. Man. Cybern. Part B.* **2012**, *42*, 513–529. [[CrossRef](#)]
32. Ren, K.Q.; Pan, C.M. Collaborative localization algorithm based on dynamic correction of RSSI model parameters. *J. Huazhong Univ. Sci. Technol. (Nat. Sci. Ed.)* **2020**, *48*, 97–102. [[CrossRef](#)]
33. Indraprastha, A.; Shinozaki, M. The Investigation on Using Unity3D Game Engine in Urban Design Study. *ITB J. Inf. Commun. Technol.* **2009**, *3*, 1–18. [[CrossRef](#)]
34. Ge, X.; Xie, J.C.; Wang, X.W.; Liu, Y.; Shi, H.B. A virtual adjustment method and experimental study of the support attitude of hydraulic support groups in propulsion state. *Measurement* **2020**, *158*, 1–13. [[CrossRef](#)]
35. Xie, J.C.; Yang, Z.J.; Wang, X.W.; Zeng, Q.; Li, J.L.; Li, B. A Virtual Reality Collaborative Planning Simulator and its Method for Three Machines in a Fully Mechanized coal Mining Face. *Arab. J. Sci. Eng.* **2018**, *43*, 4835–4854. [[CrossRef](#)]